Faraday effect in a short pulse propagating in a resonant medium under an ultra-strong magnetic field

J. G. Huang (黄俊刚), G. Slavcheva, and O. Hess

Advanced Technology Institute, Faculty of Engineering and Physical Sciences, University of Surrey, Guildford, GU2 7XH Surrey, United Kingdom

We propose a dynamical model for description of the nonlinear Faraday rotation experienced by a short pulse propagating in a resonant medium subject to an ultra-strong static magnetic field. Under the assumptions of a sufficiently strong external magnetic field, such that the Zeeman splitting of the quantum system energy levels is large compared to the linewidth of the optical transitions involved and the bandwidth of the incident light, the light effectively interacts with a two-level system. Our numerical simulations show that the Faraday effect under these conditions is significantly distinctive from the one caused by weak to moderately strong magnetic field. Nonlinear coherent effects such as inhomogeneous polarization rotation along the pulse duration and an onset of a circularly polarized stimulated emission and coherent ringing have been demonstrated. Some views on the experimental observation of the predicted phenomena are given.

I. INTRODUCTION

It is well known that the polarization direction of linearly polarized light continuously rotates while it passes through certain materials such as solutions of chiral molecules, solids with rotated crystal planes, and spin-polarized gases. This phenomenon of polarization plane rotation during propagation is called optical activity. When placed in a magnetic field aligned in the propagation direction of the linearly polarized light, all atoms and molecules exhibit optical activity. The magnetic-field-induced optical activity is named after its discoverer Michael Faraday as the Faraday effect.

While it commonly occurs in the transparent spectrum of a medium, the Faraday effect can be observed in the absorptive or nontransparent spectrum region via self-induced transparency. Self-induced transparency is a phenomenon whereby optical pulses propagate through a resonant absorptive medium without energy loss or distortion. Courtens[1] predicted that a linearly polarized 2π pulse will undergo the giant Faraday rotation accompanied by no absorption when propagating in a resonant medium having the Zeeman splitting of the resonant energy levels.

The investigation of the Faraday effect in a resonant medium is of considerable interest for nonlinear optical spectroscopy, since it provides important information about the level structure of the quantum system, including the set of closely lying sublevels, due to the Zeeman splitting in an external magnetic field. The nonlinear Faraday rotation in a medium exhibiting optically induced circular birefringence has been suggested as a mechanism for achieving a stable polarization mode locking of a soliton laser.[2] On the other hand, the magneto-optic Faraday effect allows measurement of the magnetic moment dynamics on an ultrafast time scale and with high spatial resolution. The time-resolved Faraday rotation spectroscopy, in particular, employs pump-probe techniques to prepare and/or detect a spin population by using a train of ultrashort optical pulses at a resonance frequency tuned just above the absorption edge of a semiconductor. It represents a powerful technique for measuring spin

coherence in semiconductors, initially used to study the magnetization dynamics in bulk magnetic semiconductors[3] and quantum wells.[4,5] The more recent application of the time-resolved Faraday effect to nonmagnetic semiconductors strikingly reveals long spin coherence times in bulk semiconductors[6] and ensembles of electron spins in quantum dots (QDs).[7–9] Measured rotation angles, however, are usually quite small ($\sim \mu$rad in bulk GaAs at room temperature[10]) which makes the detection of single electron spins difficult. Nevertheless, observation of Faraday rotation from a time-averaged single spin state of a single electron confined in a QD has been recently reported.[9] In this respect, the giant Faraday rotation predicted by Courtens in resonant media in the self-induced transparency regime could be used as a probe of the single confined spin dynamics, in view of quantum computation applications.

Most analyses[1,11–13] of the Faraday effect in a resonant medium consider the situation when the magnetic field is weak so that the width of the Zeeman splitting is (much) smaller than the linewidth of the incident light. With the strength of magnetic field on this order of magnitude, it is necessary to use a system of four levels or more (depending on the angular momentum quantum number of the relevant levels) to describe the medium. However, if the magnetic field is so strong that the magnitude of the Zeeman splitting is much larger than the linewidth of the relevant transitions and the bandwidth of the incident light, the light cannot be resonant with more than one transition (Fig. 1). We refer to the magnetic field that can induce the Zeeman splitting satisfying this condition as an ultra-strong. Under such a magnetic field, if the central frequency of the incident light is tuned with the resonant frequency of a transition with $\Delta M = 1$ or $\Delta M = -1$ (ΔM represents the magnetic quantum number difference between the upper level and the lower level of the transition), the effect from this transition on the incident light will be much larger than that from other transitions and the interaction of the light with the medium can be effectively considered as an interplay of the light with a two-level medium.
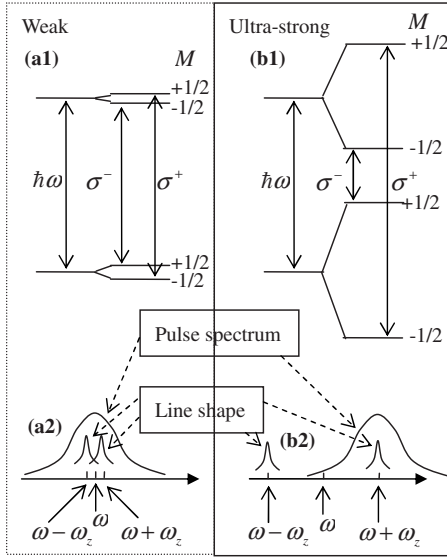
FIG. 1. Energy level diagram of a resonant two-level system (Kramers doublet depicted for simplicity) which splits into the Zeeman sublevels in (a1) applied weak to moderate magnetic field and the same system from (a1) in (b1) applied ultra-strong magnetic field. (a2) Pulse spectrum and linewidths correspond to the system in (a1) and (b2) pulse spectrum and linewidths correspond to the system in (b1).

In this paper, we consider the Faraday effect in a resonant absorptive medium under an ultra-strong magnetic field. More specifically, we investigate the Faraday rotation of a 2π pulse and show that its characteristics are significantly different from those in a weak (to moderately strong) magnetic field. Some suggestions for experimental observation of the predicted phenomena are also given.

II. THEORETICAL MODEL

Consider a linearly polarized laser pulse propagating in a resonant medium along the direction of an ultra-strong magnetic field. Under the above mentioned conditions, the light-medium interaction can be effectively described by the interaction of the light with a two-level quantum system. The system Hamiltonian $\mathbf{H} = \mathbf{H}_0 - \mathbf{p} \cdot \mathbf{E}$ is composed of an unperturbed part $\mathbf{H}_0$ which determines the energy separation of the two levels, and an interaction Hamiltonian in dipole approximation $\mathbf{H}_{int} = -\mathbf{p} \cdot \mathbf{E}$, where $\mathbf{p}$ and $\mathbf{E}$ are the electric dipole moment operator and the light electric field vector, respectively.[14–17] Here, we only consider the case of $\Delta M = 1$ transition; the case of $\Delta M = -1$ can be analogously treated. When denoting the propagation direction as z, the system Hamiltonian for $\Delta M = 1$ transition can be written as[18,19]

$$\mathbf{H} = \begin{pmatrix} 0 & -\dfrac{\gamma}{2}(E_x - iE_y) \\ -\dfrac{\gamma}{2}(E_x + iE_y) & \hbar\omega_0 \end{pmatrix}, \quad (1)$$

where ω_0 is the transition frequency, γ the dipole transition matrix element, and E_x and E_y are the x and y components of the light electric field vector, respectively.

The dynamical evolution of the system can then be determined by the Liouville equation $i\hbar \partial\rho/\partial t = [\mathbf{H}, \rho]$ for the density operator ρ in the Hilbert space. To simplify the analysis and to couple the time-evolution equations to the Maxwell curl equations for the real E- and H-field components, we use the real pseudospin vector,[15,18–21] $\mathbf{S} \equiv (S_1, S_2, S_3) \equiv [\text{Tr}(\rho\sigma_1), \text{Tr}(\rho\sigma_2), \text{Tr}(\rho\sigma_3)]$, instead of the complex density matrix ρ to describe the system evolution (σ_1, σ_2, and σ_3 are the Pauli matrices). One can derive from the Liouville equation the equation of motion for $\mathbf{S}$,[15,19–21]

$$\frac{\partial S_1}{\partial t} = \omega_0 S_2 - \frac{\gamma}{\hbar} E_y S_3 - \frac{(S_1 - S_{10})}{T_2}, \quad (2a)$$

$$\frac{\partial S_2}{\partial t} = -\omega_0 S_1 + \frac{\gamma}{\hbar} E_x S_3 - \frac{(S_2 - S_{20})}{T_2}, \quad (2b)$$

$$\frac{\partial S_3}{\partial t} = \frac{\gamma}{\hbar} E_y S_1 - \frac{\gamma}{\hbar} E_x S_2 - \frac{(S_3 - S_{30})}{T_1}. \quad (2c)$$

Here, we have introduced phenomenological relaxation times T_1 and T_2 to represent population relaxation and polarization dephasing, respectively. (S_{10}, S_{20}, S_{30}) is the equilibrium value of the vector. The equilibrium value of an absorptive medium is usually set to be $(0, 0, -1)$. One benefit of using the pseudospin vector is that its components are related to the real physical quantities: S_1 and S_2 represent, respectively, the dispersive and absorptive components of the polarization; S_3 corresponds to the fractional population difference of the two energy levels.[16]

The macroscopic polarization density induced in the medium can be calculated by using $\mathbf{P} = -N\langle \mathbf{p} \rangle = -N\,\text{Tr}(\rho\mathbf{p})$, where N is the resonant dipole density. Because $\mathbf{p} = \gamma/2(\hat{x}\sigma_1 + \hat{y}\sigma_2)$ ($\hat{x}$ and $\hat{y}$ are, respectively, unit vectors along x and y coordinate axes),[14,19] the x and y components of the polarization vector, P_x and P_y, can be calculated from S_1 and S_2, similar to the general procedure described in Ref. 19,

$$P_x = -\frac{1}{2} N\gamma S_1, \quad (3a)$$

$$P_y = -\frac{1}{2} N\gamma S_2. \quad (3b)$$

The z component of the polarization vector is always 0.

In one-dimensional media, the evolution of the electric vector $(E_x, E_y, 0)$ and magnetic vector $(H_x, H_y, 0)$ of light is described by the Maxwell equations,

$$\frac{\partial H_x(z,t)}{\partial t} = \frac{1}{\mu} \frac{\partial E_y(z,t)}{\partial z}, \quad (4a)$$

$$\frac{\partial H_y(z,t)}{\partial t} = -\frac{1}{\mu} \frac{\partial E_x(z,t)}{\partial z}, \quad (4b)$$

$$\frac{\partial E_x(z,t)}{\partial t} = -\frac{1}{\varepsilon} \frac{\partial H_y(z,t)}{\partial z} - \frac{1}{\varepsilon} \frac{\partial P_x(z,t)}{\partial t}, \quad (4c)$$
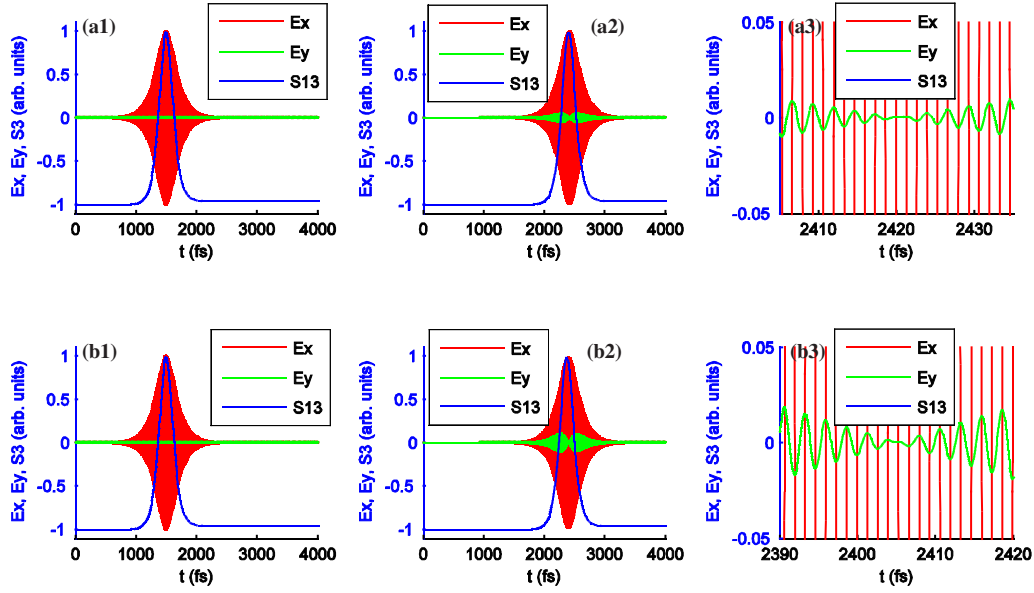
FIG. 2. (Color online) Evolution of a 2π pulse in a resonant absorbing medium (upper row: $N=1.0\times10^{19}$ m^{-3}, lower row: $N=2.0\times10^{19}$ m^{-3}): [(a1) and (b1)] $z=0$ μm; [(a2) and (b2)] $z=280$ μm; (a3) blowup of the center portion of (a2); and (b3) blowup of the center portion of (b2). (Note that E_x and E_y are normalized with respect to E_0.)

$$\frac{\partial E_y(z,t)}{\partial t} = \frac{1}{\varepsilon}\frac{\partial H_x(z,t)}{\partial z} - \frac{1}{\varepsilon}\frac{\partial P_y(z,t)}{\partial t}. \tag{4d}$$

The initial pulse (the pulse at the entrance facet $z=0$ of the medium) has the following expression:

$$\mathbf{E}(z=0,t) = A_x(t)\cos(\omega_0 t)\hat{\mathbf{x}} + i\hat{\mathbf{y}}0. \tag{5}$$

For simplicity, we only investigate the propagation of a 2π pulse with

$$A_x(t) = E_0 \operatorname{sech}\left(\frac{t-t_0}{\tau}\right), \tag{6}$$

where

$$E_0 = \frac{4\hbar}{\gamma\tau}, \tag{7}$$

τ is the pulse width and t_0 is a time offset.

III. NUMERICAL RESULTS AND DISCUSSION

Since Eqs. (2) and (3) combined with Eq. (4) and boundary condition (5) cannot be analytically solved, we use the finite difference time domain method to numerically solve the system. We consider a 2π hyperbolic secant (sech) pulse with a central wavelength $\lambda=800$ nm and $\tau=150$ fs propagating in a 300 μm long medium with refractive index $n=1.0029$ and dipole coupling $\gamma=4.8\times10^{-28}$ C m. To numerically achieve a 2π pulse, we use the technique from Ref. 16 to compensate for the energy discrepancy between a theoretical 2π pulse and a numerical one, i.e., setting $t_0=10\tau$ and dividing E_0 by $\arctan(\sin u)|_{-10}^{10}$. We also set $T_1=100$ ps and $T_2=10$ ps so that the system satisfies the (sharp-line limit) condition of self-induced transparency, $T_1, T_2 \gg \tau$. The upper and lower rows of Fig. 2 show the pulse shapes and popula-

tion difference profiles for $N=1.0\times10^{19}$ and $N=2.0\times10^{19}$ m^{-3}, respectively. One can see that, when propagating across the medium, the initial linearly polarized pulse [Figs. 2(a1) and 2(b1)] becomes elliptically polarized [Figs. 2(a2) and 2(b2)] and the Faraday rotation along the pulse duration is inhomogeneous. The blowups of the central portion of the pulse at $z=280$ μm [Figs. 2(a3) and 2(b3)] illustrate that, in time coordinate, the amplitude A_y of E_y is zero at the peak of the pulse (denoting the peak time as $t=t_p$). Figures 2(a2) and 2(b2) show that, in the vicinity of the peak point, A_y is a nonmonotonic function, initially increasing in absolute value with the increase in $|t-t_p|$, reaching a maximum, and subsequently decreasing. However, we should note that A_y is an antisymmetric function of the relative (with respect to the peak value t_p) time.

These phenomena can be understood by simple analysis of the governing equations. Figure 2 suggests that, during the initial propagation ($z\approx0$), the change in the E_x component of the pulse is very insignificant and the E_y component is small compared to E_x. Therefore, as a good approximation, one can consider that the field seen by the two-level resonant dipoles near the entrance facet $z=0$ has the form

$$\mathbf{E} = E_0 \operatorname{sech}[(t'-t_0)/\tau][\hat{\mathbf{x}}\cos(\omega_0 t') + i\hat{\mathbf{y}}0], \tag{8}$$

where $t'=t-z/V$ (V is the pulse propagation velocity[15]).

Under the rotating wave approximation and in the sharp-line limit ($T_1\gg\tau$ and $T_2\gg\tau$), the pseudospin vector in rotating frame coordinates (u,v,w), excited by $\mathbf{E}$, has the following expression:[15]

$$u = 0, \tag{9a}$$

$$v = 2\operatorname{sech}\left(\frac{t'-t_0}{\tau}\right)\tanh\left(\frac{t'-t_0}{\tau}\right), \tag{9b}$$

$$w = -1 + 2\,\text{sech}^2\left(\frac{t'-t_0}{\tau}\right). \tag{9c}$$

Therefore, a rotation transform gives

$$S_1 = 2\,\text{sech}\left(\frac{t'-t_0}{\tau}\right)\tanh\left(\frac{t'-t_0}{\tau}\right)\sin(\omega_0 t'), \tag{10a}$$

$$S_2 = 2\,\text{sech}\left(\frac{t'-t_0}{\tau}\right)\tanh\left(\frac{t'-t_0}{\tau}\right)\cos(\omega_0 t'), \tag{10b}$$

$$S_3 = -1 + 2\,\text{sech}^2\left(\frac{t'-t_0}{\tau}\right). \tag{10c}$$

Combining Eqs. (4a) and (4d), one obtains

$$\frac{\partial^2 E_y}{\partial t^2} = -\frac{1}{\varepsilon\mu}\frac{\partial^2 E_y}{\partial z^2} - \frac{1}{\varepsilon}\frac{\partial^2 P_y}{\partial t^2}. \tag{11}$$

Changing variables according to $t'' = t - z/K$ (K is a constant), Eq. (11) becomes

$$\left(1 + \frac{1}{K^2\varepsilon\mu}\right)\frac{\partial^2 E_y}{\partial t''^2} + \frac{\partial^2 E_y}{\partial t\partial t''} + \frac{\partial^2 E_y}{\partial t''\partial t} + \frac{\partial^2 E_y}{\partial t^2}$$
$$= -\frac{1}{\varepsilon}\left[\frac{\partial^2 P_y}{\partial t''^2} + \frac{\partial^2 P_y}{\partial t\partial t''} + \frac{\partial^2 P_y}{\partial t''\partial t} + \frac{\partial^2 P_y}{\partial t^2}\right]. \tag{12}$$

When z is very small or when K is very large, $t'' \approx t$ and Eq. (12) is equivalent to

$$\left(4 + \frac{1}{K^2\varepsilon\mu}\right)\frac{\partial^2 E_y}{\partial t^2} \approx -\frac{4}{\varepsilon}\frac{\partial^2 P_y}{\partial t^2}. \tag{13}$$

Because the light propagation speed in the medium is given by $1/\sqrt{\varepsilon\mu}$, t and $z\sqrt{\varepsilon\mu}$ usually have the same order of magnitude, and the approximation $t'' \approx t$ could be made only when $K \gg 1/\sqrt{\varepsilon\mu}$. Therefore, Eq. (13) can be written down in the following approximation form:

$$\frac{\partial^2 E_y}{\partial t^2} \approx -\frac{1}{\varepsilon}\frac{\partial^2 P_y}{\partial t^2}. \tag{14}$$

Integrating twice Eq. (14) and using the initial condition $E_y(z,0) = P_y(z,0) = 0$ and boundary condition $E_y(0,\infty) = P_y(0,\infty) = 0$, we get

$$E_y = -P_y/\varepsilon. \tag{15}$$

Combining Eqs. (3b) and (10b), with Eq. (15), we get

$$E_y = \frac{N\gamma}{\varepsilon}\,\text{sech}\left(\frac{t'-t_0}{\tau}\right)\tanh\left(\frac{t'-t_0}{\tau}\right)\cos(\omega_0 t'). \tag{16}$$

This expression is valid when the amplitude of E_y is very small compared to that of E_x, and this condition is satisfied within a very short time interval after the pulse enters the resonant medium. The above analysis shows that, as long as these assumptions are valid, A_y will always have a zero point when $t = z/V + t_0$. This is significantly different from the Faraday effect of a 2π pulse under a weak magnetic field.[1,11] From Eq. (2) in Ref. 11, the rotation angle θ under weak magnetic field can be calculated by $\theta = Az$, where A is a con-
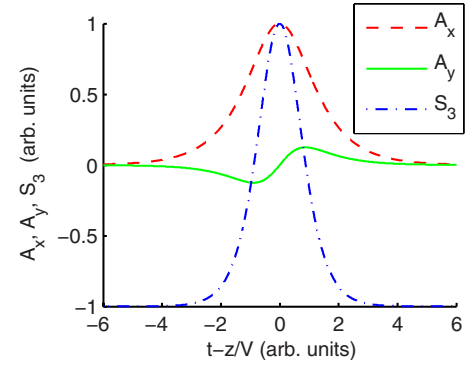
FIG. 3. (Color online) Schematic plot of $A_x = \text{sech}(t - z/V)$, $A_y = 0.25\,\text{sech}(t - z/V)\tanh(t - z/V)$, and $S_3 = -1 + 2\,\text{sech}^2(t - z/V)$.

stant depending on the system parameters such as dipole density and pulse width, but independent of time and position. So, for an initial pulse given by Eq. (5), the E_y component will have the expression: $E_y = E_0 \sin(Az)\text{sech}[(t' - t_0)/\tau]\cos(\omega_0 t')$. So, when $t = z/V + t_0$, the amplitude of E_y always reaches its maximum, $E_0 \sin(Az)$.

Although Eq. (16) is only valid in an infinitesimal time interval after the pulse enters the medium, it can still assist our understanding of the initial evolution tendency of the E_y component. Figure 3 is a schematic plot of $A_x = \text{sech}(t - z/V)$, $A_y = 0.25\,\text{sech}(t - z/V)\tanh(t - z/V)$, and $S_3 = -1 + 2\,\text{sech}^2(t - z/V)$. It is qualitatively similar to the amplitude profiles in Figs. 2(a2) and 2(b2). Equation (16) successfully predicts that A_y at two sides of the peak time $t' = t_0$ are symmetric in amplitude but have opposite signs [consistent with Figs. 2(a3) and 2(b3)]. It also indicates that the two extrema of A_y correspond to the two absolute value maxima of E_y along the pulse duration [see Figs. 2(a2) and 2(b2)].

Figure 4 shows the field and population inversion profiles at three different positions (columns) for three different dipole densities (rows). From all three rows, one can discern a common phenomenon: the magnitude of the E_y component increases with the increase in the propagation distance. For a relatively low dipole density, $N = 2.0 \times 10^{19}$ m^{-3} (first row), at $z = 48$ μm, the population difference exhibits an approximately symmetric profile with a maximum nearly aligned with the pulse peak point [see Fig. 4(a1)]. With the increase in z, the peak point of the population difference profile shifts toward the tail of the pulse [see Figs. 4(a2) and 4(a3)]. Increasing the dipole density can make this shift more severe at the same position. For $N = 2.5 \times 10^{20}$ m^{-3} (second row), the shift is already very obvious at $z = 48$ μm [see Fig. 4(b1)], leading to a change in the pulse shape of the E_x component and eventually splits the main pulse into two [see Figs. 4(b2) and 4(b3)]. This pulse splitting phenomenon cannot be observed in weak (or moderately strong) magnetic field where a 2π pulse is predicted to propagate undistorted.[1,11]

Comparing figures in each column in Fig. 4, one can notice that the increase in dipole density increases the speed of growth of the E_y component, and, with the increase in N, the coherent stimulated emission (resonance florescence)[22] after the main pulse also becomes apparent. The coherent ringing,[23] which is an important signature of the coherent emission, becomes much more significant when N increases.
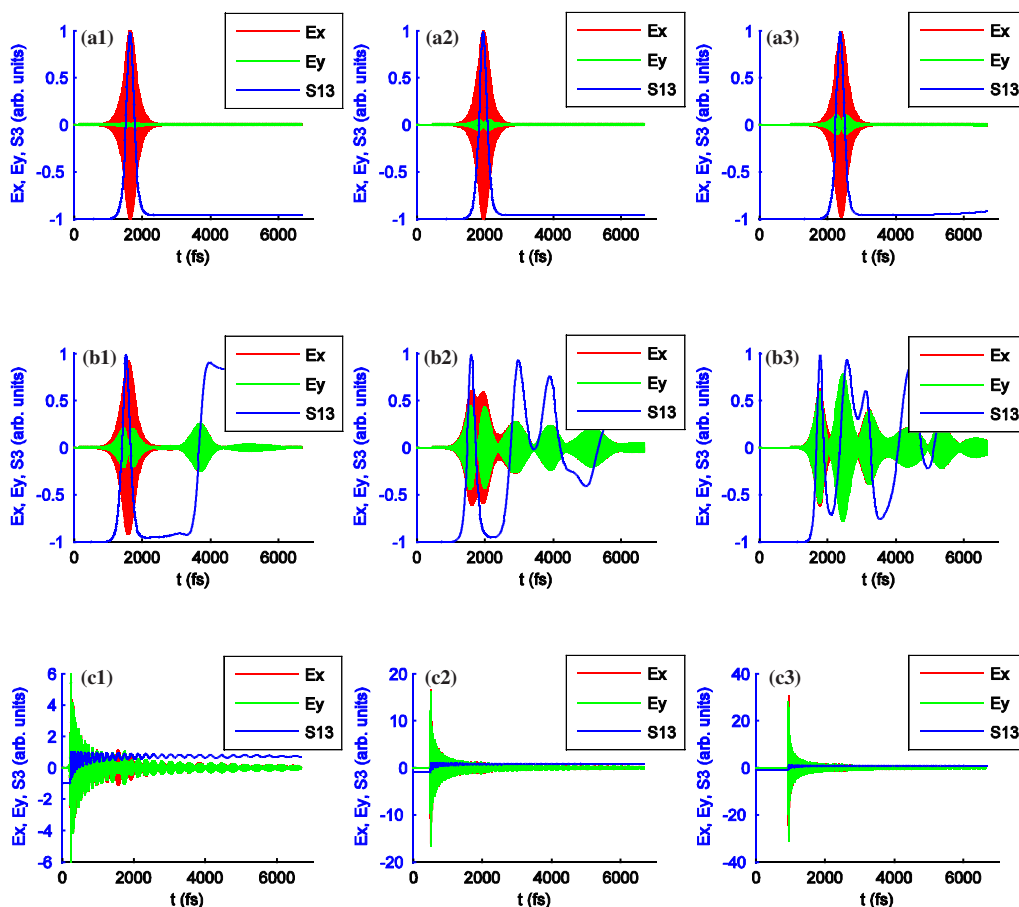
FIG. 4. (Color online) Evolution of a 2π pulse in a medium with different atom densities (first row: $N=2.0\times10^{19}$ m^{-3}; second row: $N=2.5\times10^{20}$ m^{-3}; and third row: $N=2.5\times10^{22}$ m^{-3}) at [(a1), (b1), and (c1)] $z=48$ μm, [(a2), (b2), and (c2)] $z=144$ μm, and [(a3), (b3), and (c3)] $z=280$ μm. (Note that E_x and E_y are normalized with respect to E_0.)

The third row illustrates that, for a relatively large N, the coherent emission appears to be more and more pronounced with the increase in z and eventually becomes the dominant effect. Further increase in the dipole density can make this process faster. The dependence of the coherent emission on the system parameters and how the enhanced coherent emission destroys self-induced transparency will be discussed in a separate paper. Since the coherence emission from a $\Delta M = \pm 1$ transition is always circularly polarized, the increase in coherent emission with increasing the propagation distance z indicates that the field tends to be a circularly polarized wave when propagating further away. This tendency can be seen in all three rows.

IV. SOME VIEWS ON EXPERIMENTAL OBSERVATION

To observe the phenomena predicted in the above simulation, the experimental system should first satisfy the conditions for self-induced transparency observation. These include that (1) the central frequency of the incident sech pulse should be nearly resonant with the transition frequency and (2) the pulse duration should be much shorter than the population relaxation and polarization dephasing times. Besides these conditions, the observation of the predicted phenomena requires that the Zeeman splitting of the relevant energy lev-

els should be large enough, so that the differences of the intrinsic frequencies of nearby transitions are much larger than the linewidth of the dipole optical transitions involved and the bandwidth of the incident light.

It is well known that the self-induced transparency has already been observed in atomic vapors,[24] erbium-doped waveguides,[25] and semiconductors.[26] In principle, all these three kinds of systems can be used to observe the phenomena predicted here provided that the available magnetic field is strong enough to induce a sufficiently large Zeeman splitting. However, the following analysis indicates that the semiconductor system might be the most convenient one among them for the observation of the predicted phenomena.

Due to many broadening effects such as the Doppler effect, atomic vapors will usually have much larger linewidth than that of a solid-state system. A magnetic field that is stronger than the maximum magnetic field available in laboratory may be needed to satisfy the condition for the Zeeman splitting, although some techniques such as replacing the vapor cell by an atomic beam[24] can be used to reduce the broadening effects.

In the erbium-doped fiber system, because of the small magnitude (1.4×10^{-32} C m) (Ref. [25]) of the dipole moment constant and the limitation of the doping density, a medium length on the scale of meters might be necessary to produce

significant rotation for observation. To generate an ultra-strong, uniform static magnetic field on such a length scale will bring inconveniences to experiments.

Semiconductors usually have larger dipole moments than that of the atoms in the erbium-doped fiber systems. For example, the dipole moment of GaAs is on the order of 10^{-28} C m. On the other hand, the dipole density in a semiconductor increases with the optical excitation intensity. Therefore, a relatively short medium length (on the scale of microns or smaller) is sufficient to produce significant rotation for observation. Furthermore, in a bound exciton state (such as in CdS)[26] or in an excitonic state of a quantum well or a quantum dot, the quantum levels can be considered as atomiclike levels and some of them have a small linewidth. All these characters make some carefully selected semiconductor systems the most convenient choice for the observation of the phenomena predicted above. One example of these systems is the GaAs/Al$_x$Ga$_{1-x}$As quantum well or superlattice.[27]

According to the photocurrent spectrum of the GaAs/Al$_x$Ga$_{1-x}$As superlattice (Fig. 4 of Ref. 27), under an 8 T magnetic field, the 2s electron-heavy-hole transition has a Zeeman splitting energy of 2.5 meV. If we assume a linear increase in the splitting energy with the magnetic field, a 40 T magnetic field, which is slightly lower than the maximum magnetic field currently available in laboratory, will lead to a 12.5 meV splitting energy. The measurement in Ref. 27 indicates that under applied electric field of 9 V/cm, the two resulting states have linewidths of about 2.2 and 2.4 meV. However, the linewidth should be much smaller without an applied electric field. Therefore, considering an experiment by using a sech pulse with a full width at half maximum of several picoseconds (say 6 ps), based on a normal minimum time-bandwidth product of 0.32 for a sech pulse,[28] a pulse of 6 ps duration would have a bandwidth of $\Delta\omega = 0.32/6 \times 10^{-12} \approx 5.33 \times 10^{11}$ Hz, which translates into energy units as $\Delta E = 5.33 \times 10^{11}/2.418 \times 10^{14} \approx 2.2$ meV. For an unbiased system with magnetic field of 40 T applied, this pulse can be considered to approximately satisfy the condition for observation of these predicted phenomena.

V. CONCLUSIONS

We have presented a model for describing Faraday rotation when the Zeeman splitting induced by the magnetic field is much larger than the linewidth of the relevant transitions and the bandwidth of the incident light. Numerical investigation shows that the Faraday effect under this condition is significantly different from that caused by weak (to moderately strong) magnetic field. Some views on the experimental observation of the predicted phenomena are given.

Since the nonlinear Faraday rotation in a resonant medium under weak (to moderately strong) magnetic field can be considered as a resonant coherent light interaction with discrete multilevel systems, the special case of coherent Faraday rotation investigated here might be used as the basic building block of a more sophisticated model describing the effect in the currently experimentally accessible range of magnetic-field strengths. A thorough understanding of this simple model may facilitate the description of the Faraday effect in more complex systems.

Finally, we want to point out one limitation of this model. The present model assumes that the contributions from other transitions can be neglected due to the applied ultra-strong magnetic field. Because the magnitude of the applied magnetic field can only enter the model through the magnitude of the Zeeman splitting of the relevant energy levels, and within the two-level model this information is no longer available, neglecting the contributions from other transitions in this model simplifies the analysis at the cost of losing the information of the magnitude of the applied magnetic field. Therefore, it is impossible to represent the Faraday rotation as a function of the applied magnetic field by using this simplified model. To describe the quantitative relationship between the Faraday rotation and the applied magnetic field, one needs to extend this model to include contributions from at least one more transition. Work in this direction is currently underway.

ACKNOWLEDGMENT

[1] E. Courtens, Phys. Rev. Lett. **21**, 3 (1968).

[2] S. Wabnitz, E. Westin, R. Frey, and C. Flytsanis, J. Opt. Soc. Am. B **13**, 2420 (1996).

[3] D. D. Awschalom, J. M. Halbout, S. von Molnar, T. Siegrist, and F. Holtzberg, Phys. Rev. Lett. **55**, 1128 (1985).

[4] J. J. Baumberg, D. D. Awschalom, N. Samarth, H. Luo, and J. K. Furdyna, Phys. Rev. Lett. **72**, 717 (1994).

[5] T. Ostreich, K. Schonhammer, and L. J. Sham, Phys. Rev. Lett. **75**, 2554 (1995).

[6] J. M. Kikkawa and D. D. Awschalom, Phys. Rev. Lett. **80**, 4313 (1998).

[7] X. Marie, T. Amand, P. Le Jeune, M. Paillard, P. Renucci, L. E. Golub, V. D. Dymnikov, and E. L. Ivchenko, Phys. Rev. B **60**, 5811 (1999).

[8] J. A. Gupta and D. D. Awschalom, Phys. Rev. B **63**, 085303 (2001).

[9] A. Greilich, R. Oulton, E. A. Zhukov, I. A. Yugova, D. R. Yakovlev, M. Bayer, A. Shabaev, Al. L. Efros, I. A. Merkulov, V. Stavarache, D. Reuter, and A. Wieck, Phys. Rev. Lett. **96**, 227401 (2006).

[10] A. V. Kimel, F. Bentivegna, V. N. Gridnev, V. V. Pavlov, R. V. Pisarev, and T. Rasing, Phys. Rev. B **63**, 235201 (2001).

[11] B. D. Silverman and J. C. Suits, Phys. Rev. A **6**, 847 (1972).

[12] R. Serber, Phys. Rev. **41**, 489 (1932).

[13] B. M. Harvey and F. C. Spano, J. Opt. Soc. Am. B **11**, 1177 (1994).

[14] S. L. McCall and E. L. Hahn, Phys. Rev. **183**, 457 (1969).

[15] L. Allen and J. H. Eberly, *Optical Resonance and Two-Level Atoms* (Wiley, New York, 1987).

[16] R. W. Ziolkowski, J. M. Arnold, and D. M. Gogny, Phys. Rev. A **52**, 3082 (1995).

[17] G. Slavcheva, J. M. Arnold, I. Wallace, and R. W. Ziolkowski, Phys. Rev. A **66**, 063418 (2002).

[18] R. P. Feynman, F. L. Vernon, and R. W. Hellwarth, J. Appl. Phys. **28**, 49 (1957).

[19] G. Slavcheva and O. Hess, Phys. Rev. A **72**, 053804 (2005).

[20] K. Blum, *Density Matrix Theory and Applications* (Plenum, New York, 1981).

[21] F. T. Hioe and J. H. Eberly, Phys. Rev. Lett. **47**, 838 (1981).

[22] D. C. Burnham and R. Y. Chiao, Phys. Rev. **188**, 667 (1969).

[23] D. J. Heinzen, J. E. Thomas, and M. S. Feld, Phys. Rev. Lett. **54**, 677 (1985).

[24] H. M. Gibbs and R. E. Slusher, Phys. Rev. A **6**, 2326 (1972).

[25] M. Nakazawa, Y. Kimura, K. Kurokawa, and K. Suzuki, Phys. Rev. A **45**, R23 (1992).

[26] M. Jutte, H. Stolz, and W. von der Osten, J. Opt. Soc. Am. B **13**, 1205 (1996).

[27] A. B. Hummel, T. Bauer, H. G. Roskos, S. Glutsch, and K. Kohler, Phys. Rev. B **67**, 045319 (2003).

[28] http://cmxr. com/home/education/b-w_products.htm